RSC Advances

ROYAL SOCIETY OF CHEMISTRY

www.rsc.org/advances

RSC Advances

ARTICLE

Spiroplakortone, an Unprecedented Spiroketal Lactone from the Chinese Sponge *Plakortis simplex*

Giuseppina Chianese,[a] Bin-Bin Gu,[b] Fan Yang,[b] Wei-Hua Jiao,[b] Yue-Wei Guo,[c] Hou-Wen Lin,[b,*] Orazio Taglialatela-Scafati[a,*]

A new polyketide-based metabolite, spiroplakortone (**1**), characterized as an unprecedented γ-spiroketal-γ-lactone, was obtained from the Chinese sponge *Plakortis simplex*. Structural characterization of spiroplakortone (**1**) was based on extensive spectroscopic analysis and its configuration was partly established by GIAO ^{13}C-NMR, supported by DP4 probability analysis, and ECD calculations. A plausible pathway for the biosynthesis of spiroplakortone (**1**), envisaging the formation of a carbon-carbon linkage between polyketide and aminoacid (leucine)-derived moieties, has been proposed.

Received 00th January 20xx,
Accepted 00th January 20xx

DOI: 10.1039/x0xx00000x

www.rsc.org/

1. Introduction

Marine sponges of the genus *Plakortis* (Demospongiae, Plakinidae) have been intensively investigated for their secondary metabolites over the last decades, revealing a seemingly endless parade of molecular architectures and promising bioactivities.[1] This profligacy has been related to the metabolic contribution of symbiotic microorganisms, present in large percentages in the spongal tissues,[2] although conclusive evidences unambiguously supporting this hypothesis are still elusive. The most prominent and peculiar class of *Plakortis* metabolites is given by propionate- and butyrate-based polyketides, exemplified by the simple 1,2-dioxane plakortin.[3] Plakortones[4] and simplexolides[5] are only representative examples of the many classes of plakortin-related polyketides isolated from these sponges. Their highly functionalized structures and different bioactivities have stimulated an intense research activity, including several synthetic approaches.[6,7]

Our research groups have long been involved in the investigation of *Plakortis* metabolites, leading to the discovery of new classes of polyketides, e.g. plakortethers[8] and simplextones.[9] In addition, we have disclosed the antimalarial potential of plakortin,[10] for which we have postulated a likely mechanism of action,[11] basing on the information coming from natural[12] and synthetically prepared analogues.[13]

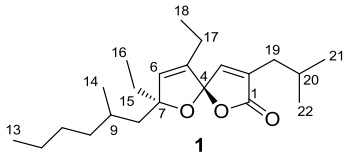

1

Fig. 1 The chemical structure of spiroplakortone (**1**).

In the course of our continuing joint analysis of a Chinese specimen of *Plakortis simplex*, aimed at characterizing its antimalarial endoperoxides,[14] we have obtained a new polyketide-based metabolite, which we named spiroplakortone (**1**), featuring a spiroketal lactone group. Herein we describe isolation, stereostructural characterization and possible biogenesis of this new compound.

2. Results and Discussion

A specimen of *Plakortis simplex* was collected along the coasts of the Xisha Islands, in the South China Sea, and exhaustively extracted with methanol. The obtained residue was successively extracted with *n*-hexane, CH_2Cl_2, EtOAc and BuOH, resulting in a concentration of the apolar polyketides into the CH_2Cl_2 phase. This was subjected to repeated column and HPLC chromatography over silica gel to afford spiroplakortone (**1**, 1.3 mg) in the pure state.

Spiroplakortone (**1**) was isolated as an optically active amorphous solid with the molecular formula $C_{22}H_{36}O_3$ (deduced by HR-ESIMS), suggesting the presence of five unsaturation degrees. The IR absorption at ν_{max} 1763 cm^{-1} was

[a] *Dipartimento di Farmacia, Università di Napoli Federico II, Via D. Montesano 49, 80131 Napoli, Italy.*
[b] *Key Laboratory for Marine Drugs, Department of Pharmacy, State Key Laboratory of Oncogenes and Related Genes, Renji Hospital, School of Medicine, c, Shanghai 200127, China*
[c] *State Key Laboratory of Drug Research, Shanghai Institute of Materia Medica, Chinese Academy of Sciences, Zu Chong Zhi Road 555, Shanghai 201203, China*

Electronic Supplementary Information (ESI) available: copies of 1D and 2D NMR spectra, tables and figures relative to computational calculations. See DOI: 10.1039/x0xx00000x

in agreement with the presence of a γ-lactone moiety. Inspection of the ^{1}H NMR spectrum (C_6D_6, Table 1) aided by the 2D HSQC NMR revealed the presence of six methyl groups (three doublets and three triplets), seven sp^3 methylenes, two sp^3 methines and two sp^2 methines (δ_H 5.35 and 6.20, both singlets), the latter likely belonging to a conjugated double bond. Additionally, the ^{13}C NMR spectrum of **1** (Table 1) included resonances of five unprotonated carbon atoms, namely a lactone carbonyl (δ_C 171.0), two additional sp^2 carbons (δ_C 137.0 and 139.5), an oxygenated sp^3 carbon (δ_C 94.5), and a deshielded sp^3 carbon resonating at δ_C 116.5. The 2D COSY spectrum of **1** was instrumental to arrange the proton multiplets within four spin systems (in bold in Figure 1): the methyl-branched chain going from H_2-8 to H_3-13, two not further coupled ethyl groups and an isobutyl group.

Table 1. NMR Data of Spiroplakortone (**1**) recorded in C_6D_6[a]

Position	δ_H, mult, *J* in Hz	δ_C, mult., *J* in Hz
1		171.0, C
2		137.0, C
3	6.20, s	144.1, CH
4		116.5, C
5		139.5, C
6	5.35, s	132.5, CH
7		94.5, C
8	1.64, , overlapped	46.4, CH_2
	1.50, m	
9	1.38, m	28.4, CH
10	1.33, m	37.9, CH_2
	1.07, m	
11	1.20, overlapped	29.0, CH_2
12	1.24, overlapped	22.9, CH_2
13	0.87, t, 7.3	14.0, CH_3
14	0.93, d, 6.8	21.7, CH_3
15	1.64, overlapped	32.2, CH_2
	1.55, overlapped	
16	0.90, t, 7.2	8.5, CH_3
17	1.74, m	18.5, CH_2
	1.58, overlapped	
18	0.82, t, 7.3	11.7, CH_3
19	2.01, dd, 12.5, 6.5	33.9, CH_2
	1.93, dd, 12.5, 6.9	
20	1.76, m	26.7, CH
21	0.71, d, 6.7	21.7, CH_3
22	0.71, d, 6.7	21.7, CH_3

[a] ^{1}H NMR: 700 MHz; ^{13}C NMR: 175 MHz

Accurate inspection of the HMBC spectrum revealed that the above four saturated chains must be attached at different positions of a bicyclic spiroketal lactone core. The network of HMBC correlations represented as red arrows in Figure 1 were instrumental to define the structure of this highly substituted bicyclic system. H-6 showed HMBC correlations with C-7, C-5 and C-4, while H-3 correlated with C-4, C-5, C-1, and C-2. Among these, the H-3/C-5 HMBC cross-peak supported the hypothesis that C-4 (δ_C 116.5) is a ketal carbon joining two ring systems, a dihydrofuran and a lactone ring, thus completing the unsaturation degrees implied by the molecular formula. The four saturated side chains could be linked at this spiroketal lactone core on the basis of key HMBC correlations, represented as blue arrows in Figure 1. Thus, both H_3-16 and H_2-8 showed HMBC cross-peaks with the oxygenated C-7; H_3-18 showed cross-peak with C-5; the isobutyl methylene protons (H_2-19) showed cross-peaks with the sp^2 unprotonated

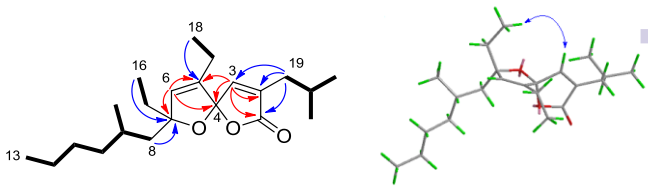

Fig. 1 COSY (boldened line) and key HMBC (colored arrows) detected for spiroplakortone (**1**). On the right structure, the arrow indicates the ROESY cross-peak between H_3-16 and H-3.

C-2, with C-3 and with the lactone carbonyl C-1. These correlations completed the assignment of the planar structure of spiroplakortone (**1**) as depicted.

The structure of spiroplakortone (**1**) includes three stereogenic centers, namely the unprotonated carbons C-4 and C-7 and the non-functionalized side chain methine C-9. The ROESY spectrum of **1** revealed the presence of a weak cross-peak between H_3-16 and H-3 (Figure 1), as the single diagnostic correlation. We decided to support this stereochemical indication by using a computational approach, through the comparison between experimental and quantum-mechanically calculated ^{13}C NMR chemical shifts.[15] To this aim, compounds showing the two possible relative orientations around the dihydrofuran ring were subjected to the initial Merck Molecular Force Field (MMFF) conformational analysis. Since the conformational arrangements of the alkyl side-chains, especially the long side chain attached at C-7, are likely to have negligible impact on the calculated ^{13}C NMR chemical shifts, our calculations were simplified by restricting the torsions around the alkyl side-chains during the conformational search. In this way, the originally resultant conformers (2,615 for 4*R**7*R** and 2,259 for 4*R**7*S**) were reduced to a single conformer for each of the two epimers (Figure 2). These conformers were re-optimized at the B3LYP/6-31G(d) level in vacuo and at the B3LYP/6-31G(d,p) level with polarizable continuum model (PCM) solvent model for benzene, which, to balance the computational accuracy and computing time, were then used in the GIAO NMR shielding constants calculations at the same level.

The computationally calculated ^{13}C NMR data of the bicyclic core of the two diastereomers (see Tables S2 and S3 of Supplementary Information) were compared to the experimental data for **1**. The two diastereomers gave relatively similar values, however, on the basis of values of CMADs (4*R**7*R** 1.3 vs 4*R**7*S** 1.1) and deviations for outliers (4*R**7*R** 2.4 vs 4*R**7*S** 1.9), the diastereomer 4*R**7*S** was found to display better overall agreement with the experimental data. The DP4 probability analyses,[16,17] using *t* distribution and DP4 database 2, also identified this diastereomer as the more likely, with a probability of 67.5% (the remaining 32.5% probability was assigned to the diastereomer 4*R**7*R**). Since we only evaluated the ^{13}C NMR chemical shifts of the bicyclic core of compound **1** for comparison, this value can be

considered acceptable. Thus, on the basis of the concurrence of experimental (ROESY) and computational evidences, we confidently assigned the 4*R**7*S** relative configuration to **1**.

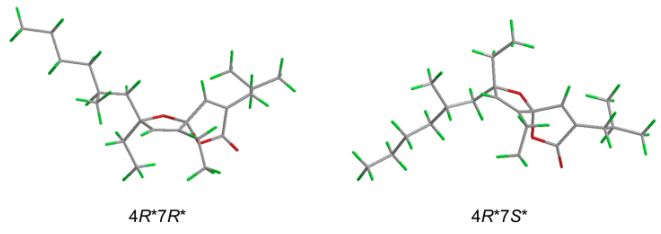

Fig. 2 Conformations of the 4*R**7*R**-**1** and 4*R**7*S**-**1** obtained by in vacuo B3LYP/6-31G(d) optimization.

To upgrade this relative configuration to the absolute one, the optimized geometry of the 4*R**7*S** stereoisomer at the B3LYP/6-31G(d) level with PCM solvent model for CH_3OH was used to perform time-dependent DFT (TDDFT) calculation. With all four functionals (B3LYP, CAM-B3LYP, BH&HLYP, PBE0) combined with TZVP basis set, the ECD spectrum was calculated (in CH_3OH) and compared with the experimental one (Figure 3).[18] This powerful and reliable computational approach is becoming increasingly important in the assignment of the absolute configuration of natural products.[19] The ECD spectrum calculated for (4*R*,7*S*)-**1** showed the same sign and almost the same magnitude of the CEs for 222 nm and 237 nm transitions. Thus, on the basis of this comparison, the 4*R*,7*S* absolute configuration was confidently assigned to compound **1**.

Unfortunately, due to the free-rotating nature of the C-7/C-8 single bond, it was not possible to establish any correlation between the configuration at C-7 and that at C-9. As expected, both experimental (ROESY, $^1H/^1H$ and $^1H/^{13}C$ coupling constants) and computational (calculation of ^{13}C or ^1H NMR chemical shifts of the side chain resonances) data were not helpful in this task. Although not experimentally demonstrated, we would propose to assign the 9*S* configuration to **1** on the basis of biogenetic considerations. Indeed, all the *Plakortis* polyketides isolated to date, including the polyketide endoperoxides previously obtained by us from the same organism,[14] have invariably shown a *S* configuration at the methyl- or ethyl-branched carbons of the "western" side chain.

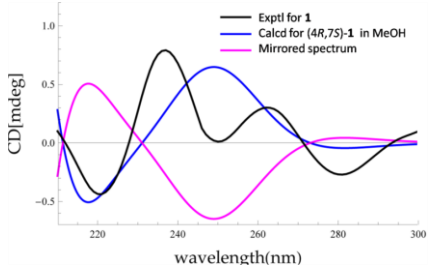

Fig. 3 Experimental ECD spectrum of compound **1** (in CH_3OH) compared with PBE0/TZVP spectrum calculated in CH_3OH (PCM model) for 4*R*,7*S*-**1** and its enantiomer.

The unprecedented spiroketal lactone skeleton of spiroplakortone (**1**) could biosynthetically result from a mixed biogenesis envisaging the formation of a carbon-carbon linkage between polyketide and aminoacid-derived moieties, as outlined in Scheme 1. A plausible polyketide precursor could be the β-ketoacid **2** (the likely ketide units are boldened), strictly related to the postulated precursor of another class of *Plakortis* metabolites, the furanylidene derivatives gracilioethers.[20] Compound **2** would undergo aldolic addition by α-ketoisocaproate (**3**), deriving from transamination of leucine and, after decarboxylation of the obtained product, a double cyclization could directly afford the target compound **1**. Spiroplakortone (**1**) was evaluated for cytotoxicity against L5178Y (mouse lymphoma) cell line using the MTT assay[21] and it exhibited a moderate activity (IC_{50} = 37.5 μM).

3. Conclusions

The unusual structural framework of spiroplakortone, including a γ-spiroketal γ-lactone functionality, coupled to its likely mixed biogenetic origin have no counterparts in the literature. These structural features can hopefully stimulate innovative synthetic approaches; the consequent availability of sufficient amounts of spiroplakortone would be instrumental to a larger exploration of its possible biological targets.

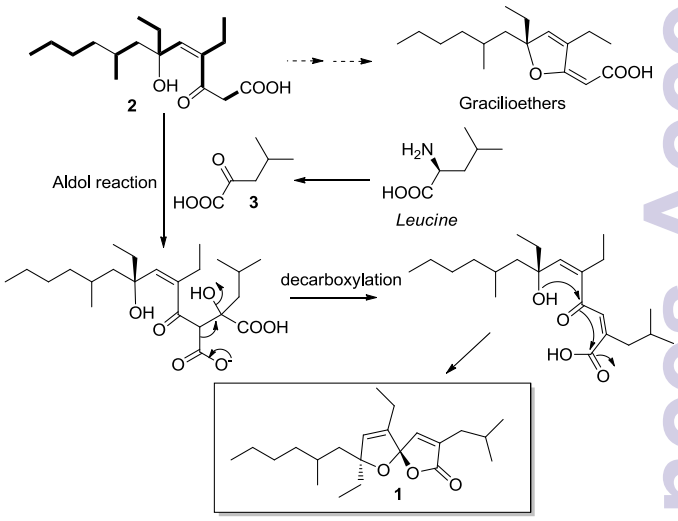

Scheme 1. Postulated biogenesis for spiroplakortone (**1**)

4. Experimental Section

4.1 General experimental procedures

Low and high resolution ESI-MS spectra were performed on a LTQ OrbitrapXL (Thermo Scientific) mass spectrometer. CD spectra were registered on a Jasco J-710 instrument. ^1H (700 MHz) and ^{13}C (175 MHz) NMR spectra were measured on Varian INOVA spectrometers. Chemical shifts were referenced to the residual solvent signal ($CDCl_3$: δ_H 7.26, δ_C 77.0; C_6D_6: δ_H 7.16, δ_C 128.4). Homonuclear ^1H connectivities were

determined by the COSY experiment. Through-space ^{1}H connectivities were evidenced using a ROESY experiment with a mixing time of 500 ms. One-bond heteronuclear ^{1}H-^{13}C connectivities was determined by the HSQC experiment; two- and three-bond ^{1}H-^{13}C connectivities by gradient-HMBC experiments optimized for a $^{2,3}J$ of 8 Hz. Medium pressure liquid chromatography was performed on a Büchi apparatus using a silica gel (230-400 mesh) column. HPLC were achieved on a Knauer apparatus equipped with a refractive index detector and LUNA (5µ, 250 × 4 mm Phenomenex) SI60 or Kinetex (2.6µ, 100 × 4.60 mm Phenomenex) C18 columns.

4.2 Animal material, extraction, isolation

A specimen of *Plakortis simplex* (order Homosclerophorida, family Plakinidae) was collected in around Xisha Island and in the South China Sea in June 2007 and identified by Prof. Jin-He Li (Institute of Oceanology, Chinese Academy of Sciences, China). A voucher sample (No. B-3) was deposited in the Laboratory of Marine Drugs, Department of Pharmacy, Changzheng Hospital. The air-dried and powdered sponge (2.0 kg, dry weight) was extracted with MeOH, and the crude extract was concentrated under reduced pressure at 45 °C to yield 500 g of residue. The residue was then extracted successively with n-hexane, CH_2Cl_2, EtOAc, and n-BuOH. Part of the dichloromethane extracts (15 g) were subjected to chromatography over silica gel column (230-400 mesh) eluting with a solvent gradient of increasing polarity from *n*-hexane to methanol. Fractions eluted with *n*-hexane/EtOAc 9:1 were further fractionated by HPLC (*n*-hexane/EtOAc 95:5, flow 0.7 mL/min) and R-HPLC (MeOH/H_2O 8:2) affording compounds **1** (1.3 mg) in the pure state.

4.3 Spiroplakortone (1)

Colorless amorphous solid; $[\alpha]_D$ -24.7 (*c* 0.01, $CHCl_3$); IR (KBr) ν_{max} 1773 cm^{-1}; UV (CH_3CN) λ_{max} (log ε): 228 (0.39), 245 (0.26) nm; ECD (CH_3CN, c = 1.00 × 10^{-3}) Δε (nm) -0.42 (222), +0.80 (237), +0.27 (266), +0.23 (283); ^{1}H and ^{13}C NMR data in C_6D_6: Table 1; ESIMS *m/z* 371.2 $[M+Na]^+$; ^{1}H NMR assignment of **1** in $CDCl_3$, 700 MHz) δ_H 6.55 (1H, bs, H-3), 5.79 (1H, bs, H-6), 2.21 (1H, dd, *J* = 14.4, 6.8 Hz, H-19a), 2.17 (1H, dd, *J* = 14.4, 6.8 Hz, H-19b), 1.96 (1H, dd, overlapped, H-17a), 1.84 (1H, dd, *J* = 16.8, 9.7 Hz, H-17b), 1.93 (1H, m, H-20), 1.68 (2H, m, H-15), 1.60 (1H, m, H-8a), 1.51 (1H, m, H-8b), 1.27 (1H, m, H-10a), 1.25 (2H, m, H-12), 1.24 (2H, m, H-11), 1.09 (3H, t, *J* = 7.2 Hz), 0.93 (3H, d, overlapped, H-21), 0.93 (3H, d, overlapped, H-22), 0.93 (3H, d, overlapped, H-14), 0.90 (3H, t, *J* = 7.1 Hz, H-16), 0.87 (3H, t, *J* = 7.0 Hz, H-13).). ^{13}C NMR assignment of **1** in $CDCl_3$ (125 MHz): δ_C 171.9 (C-1), 144.5 (C-3), 138.9 (C-5), 136.7 (C-2), 133.0 (C-6), 116.7 (C-4), 95.2 (C-7), 44.9 (C-8), 37.8 (C-10), 34.0 (C-19), 32.5 (C-15), 29.1 (C-11),28.0 (C-9), 26.8 (C-20), 22.9 (C-12), 22.1 (C-21; C-22), 22.1 (C-14), 18.3 (C-17), 14.0 (C-13), 12.1 (C-18), 8.60 (C-16). HRESIMS *m/z* 371.2569 ($[M+Na]^+$, calcd for $C_{22}H_{36}O_3Na$ 371.2562).

4.4 Computational calculations

The calculations were performed by using the density functional theory (DFT) as carried out in the Gaussian 09.[22] The preliminary conformational searches were performed with Macromodel 9.9.223.[23] Two possible structures (4*R**,7*R**-**1** and 4*R**,7*S**-**1**) of spiroplakortone (**1**) were submitted to a 3000 step Monte Carlo (MCMM) conformational search using Merck Molecular Force Field (MMFF) applying a 21 kJ/mol energy window under solvent-free conditions. The resultant 2615 conformers for 4*R**,7*R**-**1** and 2259 conformers for 4*R**,7*S**-**1** were re-clustered disregarding the orientations of all the alkyl side-chains. The only 1 corresponding conformers of 4*R**,7*R**-**1** and 4*R**,7*S**-**1** were optimized at the B3LYP/6-31G(d) level in vacuo and B3LYP/6-31G(d) level with PCM solvent model for CH_3OH. TDDFT calculations were performed in CH_3OH using various functionals (B3LYP, CAM-B3LYP, BH&HLYP, PBE0) and TZVP basis set. The pre-optimized conformations of 4*R**,7*R**-**1** and 4*R**,7*S**-**1** [B3LYP/6-31G(d) level in gas] were further optimized at the B3LYP/6-31G(d,p) level with PCM solvent model for benzene, which were then used in the GIAO NMR shielding tensors calculations at the same level. The UV and ECD spectra were generated using the program SpecDis[24] by applying a Gaussian band shape with the width of 0.33 eV, from oscillator strengths and dipole-length rotational strengths, respectively.

Computed chemical shifts were scaled empirically[25] according to the equation $\delta\_scaled\hat{}x = (\delta\_calc\hat{}x - intercept)/slope$ where δ^{x}_{calc} is the calculated chemical shift x (in ppm) relative to tetramethylsilane (TMS), which is calculated at the same level of theory, and slope and intercept are the slope and intercept resulting from a regression calculation on a plot of δ_{calc} against $\delta_{exp.}$

Acknowledgements

This research work was financially supported by EU: project Bluegenics (Grant 311848) and project IRSES (No. 246987). We also thank the financial support of China National Funds for Distinguished Young Scientists (81225023), the NSFC (Nos. 41106127, 81202441, 41476121, 81302691, and 81172978), the MOST grants (863 Projects, No. 2013AA092902) and the STCSM (Nos. 14QA1402800, 14YZ037, and 14431901300).

Notes and references

1 V. Costantino, E. Fattorusso, M. Menna, O. Taglialatela-Scafati O. *Curr. Med. Chem.* 2004, **11**, 1671-1692.
2 G. Della Sala, T. Hochmuth, R. Teta, V. Costantino, A. Mangoni. *Mar. Drugs* 2014, **12**, 5425-5440.
3 (a) M. D. Higgs, D. J. Faulkner, *J. Org. Chem.* 1978, *43*, 3451-3457. (b) E. Fattorusso, O. Taglialatela-Scafati, M. Di Rosa, A. Ianaro. *Tetrahedron* 2000, **56**, 7959-7967.
4 F. Cafieri, E. Fattorusso, O. Taglialatela-Scafati, M. Di Rosa, A. Ianaro, A. *Tetrahedron* 1999, **55**, 13831-13840.
5 X.-F. Liu, Y. Shen, F. Yang, M. T. Hamann, W.-H. Jiao, H.-J. Zhang, W.-S. Chen, H.-W. Lin. *Tetrahedron* 2012, **68**, 4635-4640.
6 H. Sugimura, S. Sato, K. Tokodume, T. Yamada. *Org. Lett.* 2014, **16**, 3384-3387.
7 P. Y. Hayes, S. Chow, F. Rahm, P. V. Bernhardt, J. J. De Voss, W. Kitching. *J. Org. Chem.* 2010, **75**, 6489-6501.

8 C. Campagnuolo, E. Fattorusso, O. Taglialatela-Scafati, A. Ianaro, B. Pisano. *Eur. J. Org. Chem.* 2002, 61-69.
9 X.-F. Liu, Y.-L. Song, H.-J. Zhang, F. Yang, H.-B. Yu, W.-H. Jiao, S.-J. Piao, W.-S. Chen, H.-W. Lin. *Org. Lett.* 2011, **13**, 3154-3157.
10 E. Fattorusso, S. Parapini, C. Campagnuolo, N. Basilico, O. Taglialatela-Scafati, D. Taramelli. *J. Antimicrob. Chemother.* 2002, **50**, 883-888.
11 O. Taglialatela-Scafati, E. Fattorusso, A. Romano, F. Scala, V. Barone, P. Cimino, E. Stendardo, B. Catalanotti, M. Persico, C. Fattorusso. *Org. Biomol. Chem.* 2010, **8**, 846-856.
12 C. Campagnuolo, E. Fattorusso, A. Romano, O. Taglialatela-Scafati, N. Basilico, S. Parapini, D. Taramelli. *Eur. J. Org. Chem.* 2007, 5077-5083.
13 E. Fattorusso, G. Campiani, B. Catalanotti, M. Persico, N. Basilico, S. Parapini, D. Taramelli, C. Campagnuolo, E. Fattorusso, A. Romano, O. Taglialatela-Scafati. *J. Med. Chem.* 2006, **49**, 7088-7094.
14 G. Chianese, M. Persico, F. Yang, H.-W. Lin, Y.-W. Guo, N. Basilico, S. Parapini, D. Taramelli, O. Taglialatela-Scafati, C. Fattorusso. *Bioorg. Med. Chem.* 2014, **22**, 4572-4580.
15 G. Bifulco, C. Bassarello, R. Riccio, L. Gomez-Paloma. *Org. Lett.* 2004, **6**, 1025-1028.
16 S. G. Smith, J. M. Goodman. *J. Am. Chem. Soc.* 2010, **132**, 12946–12959.
17 Use of the DP4 analysis is quite practical, owing to a versatile Java applet that the Goodman group has made available online. URL: http://www-jmg.ch.cam.ac.uk/tools/nmr/nmrParameters.html.
18 P. J. Stephens, J. J. Pan, K. Krohn. *J. Org. Chem.* 2007, **72**, 7641-7649.
19 Z.-F. Zhou, T. Kurtan, X.-H. Yang, A. Mandi, M.-Y. Geng, B. P. Ye, O. Taglialatela-Scafati, Y.-W. Guo. *Org. Lett.* 2014, **16**, 1390-1393.
20 M. D. Norris, M. V. Perkins, E. J. Sorensen. *Org. Lett.* 2015, **17**, 668-671.
21 J. Carmichael, W. G. De Graff, A. F. Gazdar, J. D. Minna, J. B. Mitchell *Cancer Res.* 1987, **47**, 936–942.
22 M. J. Frisch, G. W. Trucks, H. B. Schlegel, G. E. Scuseria, M. A. Robb, J. R. Cheeseman, G. Scalmani, V. Barone, B. Mennucci, G. A. Petersson, H. Nakatsuji, M. Caricato, X. Li, H. P. Hratchian, A. F. Izmaylov, J. Bloino, G. Zheng, J. L. Sonnenberg, M. Hada, M. Ehara, K. Toyota, R. Fukuda, J. Hasegawa, M. Ishida, T. Nakajima, Y. Honda, O. Kitao, H. Nakai, T. Vreven, J. A. Montgomery, J. E. Jr Peralta, F. Ogliaro, M. Bearpark, J. J. Heyd, E. Brothers, K. N. Kudin, KV. N. Staroverov, R. Kobayashi, J. Normand, K. Raghavachari, A. Rendell, J. C. Burant, S. S. Iyengar, J. Tomasi, M. Cossi, N. Rega, J. M. Millam, M. Klene, J. E. Knox, J. B. Cross, V. Bakken, C. Adamo, J. Jaramillo, R. Gomperts, R. E. Stratmann, O. Yazyev, A. J. Austin, R. Cammi, C. Pomelli, J. W. Ochterski, R. L. Martin, K. Morokuma, V. G. Zakrzewski, G. A. Voth, P. Salvador, J. J. Dannenberg, S. Dapprich, A. D. Daniels, O. Farkas, J. B. Foresman, J. V. Ortiz, J. Cioslowski, D. J. Fox. *Gaussian 09, Revision B.01*, 2010, Gaussian, Inc., Wallingford CT.
23 MacroModel, Schrödinger LLC, 2012. http://www.schrodinger.com/productpage/14/11
24 T. Bruhn, Y. Hemberger, A. Schaumlöffel, G. Bringmann. *SpecDis* version 1.50; University of Wuerzburg: Germany, 2010.
25 G. Barone, L. Gomez-Paloma, D. Duca, A. Silvestri, R. Riccio, G. Bifulco. *Chem. Eur. J.* 2002, **8**, 3233–3239.

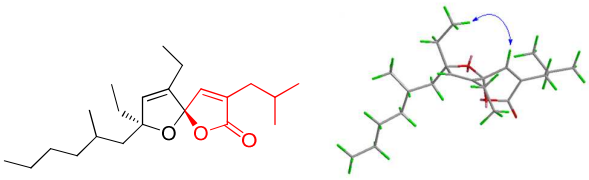

Spiroplakortone, bearing an unprecedented γ-spiroketal-γ-lactone skeleton, has been characterized basiong on extensive spectroscopic analysis, GIAO ^{13}C-NMR and ECD calculations.